arXiv:1111.1903v1 [gr-qc] 8 Nov 2011

1

Myers-Perry black holes

Robert C. Myers

In this chapter, we will continue the exploration of black holes in higher dimensions with an examination of asymptotically flat black holes with spherical horizons, *i.e.,* in d spacetime dimensions, the topology of the horizon and of spatial infinity is an S^{d-2}. In particular, we will focus on a family of vacuum solutions describing spinning black holes, known as Myers-Perry (MP) metrics. In many respects, these solutions admit the same remarkable properties as the standard Kerr black hole in four dimensions. However, studying these solutions also begins to provide some insight into the new and unusual features of event horizons in higher dimensions.

These metrics were discovered in 1985 as a part of my thesis work as a Ph.D. student at Princeton [1]. My supervisor, Malcolm Perry, and I had been lead to study black holes in higher dimensions, in part, by the renewed excitement in superstring theory which had so dramatically emerged in the previous year. We anticipated that examining black holes in $d > 4$ dimensions would be important in obtaining a full understanding of these theories. I should add that amongst the subsequent developments, this family of spinning black hole metrics was further generalized to include a cosmological constant, as well as NUT parameters.[1] While I will not have space to discuss these extensions, the interested reader may find a description of the generalized solutions in ref. [2].

1.1 Static Black Holes

Before considering spinning black holes, we should mention that the Schwarzschild solution is easily generalized to $d \geq 4$ dimensions as

$$ds^2 = -\left(1 - \frac{\mu}{r^{d-3}}\right) dt^2 + \left(1 - \frac{\mu}{r^{d-3}}\right)^{-1} dr^2 + r^2\, d\Omega^2_{d-2} \qquad (1.1)$$

[1] There is more than one such parameter in higher dimensions.

where $d\Omega_{d-2}^2$ denotes the line element on the unit (d–2)-sphere. While this vacuum solution of the d-dimensional Einstein equations was first found by Tangherlini in the early 1960's [3], it is still traditionally referred to as a Schwarzschild black hole. In part, this nomenclature probably arose because for any value of $d > 4$, the features of this spacetime (1.1) are essentially unchanged from its four-dimensional predecessor.

In particular, the constant μ emerges as an integration constant in solving the Einstein equations. In Appendix A, we derive expressions for the mass and angular momentum in a d-dimensional spacetime by examining the asymptotic structure of the metric. There one finds that μ fixes the mass of the black hole (1.1) — see eq. (1.65) — with

$$M = \frac{(d-2)\,\Omega_{d-2}}{16\pi G}\;\mu \tag{1.2}$$

where Ω_{d-2} is the area of a unit (d–2)-sphere, *i.e.,*

$$\Omega_{d-2} = \frac{2\,\pi^{\frac{d-1}{2}}}{\Gamma\big(\frac{d-1}{2}\big)}\,. \tag{1.3}$$

As long as $\mu > 0$, the surface $r^{d-3}{=}\mu$ is an event horizon. It is a straightforward exercise to generalize the discussion presented in Chapter 1 in constructing good coordinates across this surface and finding the maximal analytic extension of the geometry. The corresponding Penrose diagram then takes precisely the same form as given in Figure 1.1 of Chapter 1 where each point now represents a (d–2)-sphere.[2] Notably, there is a future (past) curvature singularity at $r = 0$ in region II (III), where $R_{\mu\nu\rho\sigma}R^{\mu\nu\rho\sigma} \propto \mu^2/r^{2(d-1)}$ as $r \to 0$. Of course, if $\mu{<}0$ the space-time has a naked time-like singularity at $r{=}0$ and the corresponding Penrose diagram matches that given in Figure 1.4 of Chapter 1.

Another simple exercise is to extend Birkhoff's theorem to higher dimensions. That is, one can solve Einstein's vacuum equations in any $d \geq 4$ with the assumption that the geometry is asymptotically flat and spherically symmetric, *i.e.,* the solution has an $SO(d-1)$ isometry, but without assuming that the spacetime is static. The Schwarzschild-Tangherlini metric (1.1) remains the most general solution and so any spherically symmetric solution of $R_{\mu\nu} = 0$ must also be static. It is also possible to prove a uniqueness theorem indicating that this metric (1.1) is the only solution of the vacuum Einstein equations in higher dimensions if one assumes that the geometry is asymptotically flat and static [4]. Hence all such static solutions are spherically symmetric and completely determined by their mass M.

[2] Of course, the past and future horizons should now be labeled as $r^{d-3}{=}\mu$.

The generalization of the four-dimensional Reissner-Nordström metric to solutions describing static charged black holes in higher dimensions is also straightforward. Again, the features of these solutions of the Einstein-Maxwell equations in $d > 4$ are essentially unchanged from those described for four dimensions in Chapter 1. Here it is interesting to extend the Majumdar-Papapetrou solutions, describing multiple extremally charged black holes in static equilibrium, to higher dimensions. With these solutions, one can construct periodic arrays of such black holes which can then be compactified using the Kaluza-Klein ansatz [5], discussed in Chapter 4. The resulting solutions provide simple analytic metrics describing black holes localized in Kaluza-Klein dimensions.

1.2 Spinning Black Holes

Before writing the metric for a spinning black hole, it is useful to first orient the discussion by writing the metric for flat space in higher dimensions. To begin, consider the case $d = 2n+1$ (with $n \geq 2$), in which case the flat space metric can be written as

$$\begin{aligned} ds^2 &= -dt^2 + \sum_{i=1}^{n} \left(dx_i^2 + dy_i^2 \right) \\ &= -dt^2 + dr^2 + r^2 \sum_{i=1}^{n} \left(d\mu_i^2 + \mu_i^2 \, d\phi_i^2 \right) . \end{aligned} \tag{1.4}$$

In the first line, we have paired all of the spatial coordinates as Cartesian coordinates (x_i, y_i) in n orthogonal planes. In the second line, we have introduced polar coordinates which can be expressed with:

$$x_i = r \, \mu_i \, \cos \phi_i \, , \qquad y_i = r \, \mu_i \, \sin \phi_i \, . \tag{1.5}$$

Implicitly, we are defining $r^2 = \sum_{i=1}^{n} \left(x_i^2 + y_i^2 \right)$ and so the direction cosines μ_i are constrained to satisfy

$$\sum_{i=1}^{n} \mu_i^2 = 1 \, . \tag{1.6}$$

Hence not all of the $d\mu_i^2$ in the flat space metric (1.4) are independent and one of these terms can be eliminated using this constraint. However, we have left this replacement implicit for the sake of keeping the metric simple. For completeness, we note that the range of each of the coordinates is: $t \in (-\infty, \infty)$, $r \in [0, \infty)$, $\mu_i \in [0, 1]$ and $\phi_i \in [0, 2\pi]$, where the latter are periodically identified $\phi_i = \phi_i + 2\pi$. We will adopt polar coordinates

analogous to those in eq. (1.4) to present the MP metrics for $d = 2n + 1$ below. In particular then, the black hole geometry will approach the flat space metric (1.4) asymptotically.

For an even number of dimensions, *i.e.,* $d = 2n + 2$ (with $n \geq 1$), there will be an extra unpaired spatial coordinate

$$z = r\,\alpha \qquad \text{with} \quad \alpha \in [-1, 1]\,. \tag{1.7}$$

Hence the flat space metric becomes

$$ds^2 = -dt^2 + dr^2 + r^2 \sum_{i=1}^{n} \left(d\mu_i^2 + \mu_i^2\, d\phi_i^2\right) + r^2\, d\alpha^2\,. \tag{1.8}$$

while the constraint on the direction cosines becomes

$$\sum_{i=1}^{n} \mu_i^2 + \alpha^2 = 1\,. \tag{1.9}$$

Eq. (1.8) exhibits the polar coordinates which we adopt below for the MP metric with $d = 2n + 2$.

One outstanding feature of the polar coordinates in eqs. (1.4) and (1.8) is that there are n commuting Killing vectors in the angular directions ϕ_i. The corresponding rotations in each of the orthogonal planes (1.5) match the n generators of the Cartan subalgebra of the rotation groups $SO(2n)$ or $SO(2n + 1)$ for odd and even d, respectively. This feature highlights the fact that in higher dimensions we must think of angular momentum as an antisymmetric two-tensor $J^{\mu\nu}$, *e.g.,* see eq. (1.62). In considering a general rotating body, we may simplify this angular momentum tensor by going to the center-of-mass frame, which eliminates the components with a time index. Then a suitable rotation of the spatial coordinates brings the remaining spatial components J^{ij} into the standard form

$$J^{ij} = \begin{pmatrix} 0 & J_1 & & & \\ -J_1 & 0 & & & \\ & & 0 & J_2 & \\ & & -J_2 & 0 & \\ & & & & \ddots \end{pmatrix}\,. \tag{1.10}$$

Here each of the J_i denote the angular momentum associated with motions in the corresponding plane. Note that for even d, the last row and column of the above matrix vanishes. Therefore a general angular momentum tensor is characterized by $n = \lfloor (d-1)/2 \rfloor$ independent parameters J_i. Hence the general spinning black hole metrics, which are considered below, will be specified by $n + 1$ parameters: the mass M and the n commuting angular

momenta $J^{y_i x_i}$. In four dimensions, these parameters would completely fix the black hole solution but, as we will see in section 1.2.8 and in subsequent chapters, these parameters alone will not fix a unique black hole metric in higher dimensions.

1.2.1 MP Black Hole Metrics

As can be anticipated from eqs. (1.4) and (1.8), the form of the metrics differs slightly for odd and even dimensions. Hence let us begin with the metric describing a spinning black hole in an even number of spacetime dimensions, *i.e.,* $d = 2n + 2$ with $d \geq 4$,

$$ds^2 = -dt^2 + \frac{\mu r}{\Pi F}\left(dt + \sum_{i=1}^{n} a_i \mu_i^2 \, d\phi_i\right)^2 + \frac{\Pi F}{\Pi - \mu r}\, dr^2 + \sum_{i=1}^{n} (r^2 + a_i^2)\left(d\mu_i^2 + \mu_i^2 \, d{\phi_i}^2\right) + r^2 \, d\alpha^2 \tag{1.11}$$

where

$$F = 1 - \sum_{i=1}^{n} \frac{a_i^2 \, \mu_i^2}{r^2 + a_i^2} \tag{1.12}$$

$$\Pi = \prod_{i=1}^{n} (r^2 + a_i^2)\,. \tag{1.13}$$

With $n = 1$, we have $d = 4$ and the above metric reduces to the well known Kerr solution, discussed in Chapter 1.[3] For $d = 2n+1$ with $d \geq 5$, the metric becomes

$$ds^2 = -dt^2 + \frac{\mu r^2}{\Pi F}\left(dt + \sum_{i=1}^{n} a_i \mu_i^2 \, d\phi_i\right)^2 + \frac{\Pi F}{\Pi - \mu r^2}\, dr^2 + \sum_{i=1}^{n} (r^2 + a_i^2)\left(d\mu_i^2 + \mu_i^2 \, d{\phi_i}^2\right) \tag{1.14}$$

with F and Π again given by eqs. (1.12) and (1.13). Examining the asymptotic structure of these metrics — see eq. (1.65) — one finds that the $n+1$ free parameters, μ and a_i, determine the mass and angular momentum of the black hole with

$$M = \frac{(d-2)\,\Omega_{d-2}}{16\pi G}\,\mu \tag{1.15}$$

[3] To make the connection more explicit, we would set $a_1 = a$, $\mu_1 = \sin\theta$ and $\alpha = \cos\theta$.

$$J^{y_i x_i} = \frac{\Omega_{d-2}}{8\pi G}\,\mu\, a_i = \frac{2}{d-2}\,M\, a_i$$

where Ω_{d-2} is the area of an S^{d-2} given in eq. (1.3). Setting all of the spin parameters $a_i = 0$, both eqs. (1.11) and (1.14) reduce to the d-dimensional Schwarzschild metric (1.1). Now also setting $\mu = 0$ yields the flat space metric in eqs. (1.4) and (1.8), respectively.

With general spin parameters a_i, both metrics have $n+1$ commuting Killing symmetries, corresponding to shifts in t and ϕ_i. These symmetries are enhanced when some of the spin parameters coincide. In particular, with $a_i = a$ for $i = 1, \cdots, m$, the corresponding rotational symmetry is enhanced from $U(1)^m$ to $U(m)$, where the latter acts on the complex coordinates $z_i = \mu_i e^{i\phi_i}$ in the associated subspace. A particularly interesting case is $d = 2n + 1$ with all n spin parameters equal. Then with the $U(n)$ symmetry, the solution reduces to cohomogeneity-one, *i.e.,* it depends on a single (radial) coordinate. Of course, if k of the spin parameters vanish, an $SO(2k)$ symmetry emerges in the corresponding subspace. When d is even, this enhanced rotational symmetry extends to $SO(2k + 1)$ by including the z direction.

Of course, as with the Kerr metric, these geometries are only stationary, rather than static, reflecting the rotation of the corresponding black holes. In particular, the metric components $g_{t\phi_i}$ are nonvanishing when $a_i \neq 0$ and as a result, one finds frame dragging in these higher dimensional spacetimes, just as was described in Chapter 1 for four dimensions. We might also note that eqs. (1.11) and (1.14) also contain nonvanishing $g_{\phi_i\phi_k}$. Further, implicitly there are also nonvanishing $g_{\mu_i\mu_k}$ (as well as $g_{\mu_i\alpha}$ with even d), which would appear explicitly if one of the direction cosines were eliminated with eq. (1.6) or (1.9).

1.2.2 Singularities

Various components of the metrics, (1.11) and (1.14), will diverge if either $\Pi\, F/r^\gamma = 0$ or $\Pi - \mu\, r^\gamma = 0$, where $\gamma = 2$ and 1 for d odd and even, respectively. The former indicates a true curvature singularity while the latter corresponds to an event horizon. To consider the former in more detail, one must examine a list of separate cases, *i.e.,* odd or even d and different numbers of vanishing spin parameters. In most cases, one finds that $\Pi\, F/r^\gamma = 0$ at $r = 0$ and this entire surface is singular. There are three exceptional cases which we consider in more detail below: a) even d and all $a_i \neq 0$, b) odd d and only one $a_i = 0$, and c) odd d and all $a_i \neq 0$. We should add that all of our comments with regards to curvature singularities can be confirmed by

directly examining the behaviour of the curvatures. For example, we examine the particular case of the $d = 5$ MP metric in detail in Appendix B and our results there explicitly match those discussed in (b) and (c) below.

a) even d and all $a_i \neq 0$: This case would include the Kerr metric with $d = 4$ and the results are similar to those found there, as described in Chapter 1. First it is useful here to use the constraint (1.9) to re-express eq. (1.12) as

$$F = \alpha^2 + r^2 \sum_{i=1}^{n} \frac{\mu_i^2}{r^2 + a_i^2} \quad \text{for even } d\,. \tag{1.16}$$

From this expression, we can see that in order for $\Pi\, F/r$ to vanish we must have both $r = 0$ and $\alpha = 0$. Further intuition comes from noting that it is most appropriate to think of the surfaces of constant r as describing ellipsoids of the form

$$\frac{z^2}{r^2} + \sum_{i=1}^{n} \frac{x_i^2 + y_i^2}{r^2 + a_i^2} = 1\,. \tag{1.17}$$

For example, if we set $\mu = 0$ in the black hole metric (1.11), the resulting metric describes flat space foliated by these surfaces. Hence as we approach $r = 0$, these (d–2)-dimensional ellipsoids collapse to a (d–2)-dimensional ball in the hyperplane $z = 0$. Now the direction cosine $\alpha = z/r$ acts as a radial coordinate in this ball with $\alpha = 1$ corresponding to the origin and $\alpha = 0$ being the boundary of the ball where the curvature diverges. Hence in higher even dimensions, the ring-like singularity of the Kerr metric is elevated to a singularity on a (d–3)-sphere. The (d–2)-ball at $r = 0$ acts as a two-sided aperture. Passing through the aperture to negative values of r, we enter a new asymptotically flat space with negative mass (and no horizons). Further, as noted in Chapter 1 for the Kerr metric, this region also contains closed time-like curves. Passing through the aperture a second time in the same direction, we reach a space isometric to the original $r > 0$ region and for simplicity these two regions are usually identified.

b) odd d and only one $a_i = 0$: For simplicity, let us denote the vanishing spin parameter as a_1. We begin again by rewriting eq. (1.12), this time using the constraint (1.6)

$$F = \mu_1^2 + r^2 \sum_{i=2}^{n} \frac{\mu_i^2}{r^2 + a_i^2} \quad \text{for odd } d \text{ and } a_1 = 0\,. \tag{1.18}$$

Hence in this case, for $\Pi\, F/r^2$ to vanish, we require both $r = 0$ and $\mu_1 = 0$ — note that Π contributes a factor of r^2 here. In this case, the appropriate

geometric intuition comes from regarding constant r surfaces as ellipsoids of the form

$$\frac{x_1^2 + y_1^2}{r^2} + \sum_{i=2}^{n} \frac{x_i^2 + y_i^2}{r^2 + a_i^2} = 1\,. \tag{1.19}$$

Hence as we approach $r = 0$, these (d–2)-dimensional ellipsoids collapse to a ball in the hyperplane $x_1 = 0 = y_1$. As above, μ_1 acts as a radial coordinate in this ball with $\mu_1 = 0$ corresponding to the boundary of the ball where the curvature diverges. However, a key difference from the previous case is that here as $r \to 0$, the ellipsoids (1.19) become very narrow and collapse to a point in the (x_1, y_1)-plane at $r = 0$. Hence the ball at $r = 0$ extends only in d–3 dimensions. A careful examination of the geometry shows that there is also a conical singularity in the (x_1, y_1)-plane for any $\mu_1 \neq 0$.[4] Hence the entire $r = 0$ surface is in fact singular here, although with a milder singularity than in the generic cases.

c) odd d and all $a_i \neq 0$: If we apply the constraint (1.6), eq. (1.12) becomes

$$F = r^2 \sum_{i=1}^{n} \frac{\mu_i^2}{r^2 + a_i^2} \quad \text{for odd } d\,. \tag{1.20}$$

In this case, we observe that Π approaches a finite constant at $r = 0$ and eq. (1.6) does not allow all of the μ_i can vanish simultaneously. Hence, $\Pi F/r^2$ remains finite at $r = 0$ and so there is no curvature singularity here. However, the metric (1.11) remains problematic at this location since one finds that $g_{rr} \propto r^2$ as $r \to 0$. However, this is only a coordinate singularity which is avoided by choosing a new radial coordinate $\rho = r^2$. Now in passing to negative values of ρ, the function $\Pi F/r^2(\rho)$ eventually vanishes and a curvature singularity arises at $\rho = -a_s^2$, where a_s is the absolute value of the spin parameter(s) with the smallest magnitude. If more than one spin parameter has the value $\pm a_s$, the entire surface $\rho = -a_s^2$ is singular. If only one spin parameter, say a_1, has the value $\pm a_s$, the singularity at $\rho = -a_s^2$ only appears at $\mu_1 = 0$. In this case, if $a_{s'}$ is the absolute value of the next smallest spin parameter, the geometry extends smoothly to values of $-a_{s'}^2 \leq \rho \leq -a_s^2$ in certain directions. However, the curvature singularity extends throughout this range of ρ since F can vanish for certain angular directions. Hence ultimately all trajectories moving towards smaller values of ρ end on a singularity in this region.

[4] Of course, this statement assumes that the mass parameter μ is nonvanishing.

1.2.3 Horizons

In considering the event horizons for these metrics, we must again consider separately the cases where the spacetime dimension is even or odd. Let us start with $d = 2n + 2$, which includes the Kerr metric for $d = 4$. The event horizons arise where g^{rr} vanishes and so from eq. (1.11), we require

$$\Pi - \mu r = 0\,. \tag{1.21}$$

Thus the horizons correspond to the roots of a polynomial, which is order $d - 2$ in r. Unfortunately, apart from $d = 4$ or 6, there will be no general analytic solutions (in terms of radical expressions) for the position of the horizon. Hence a complete set of necessary and sufficient conditions for the existence of a horizon is unavailable for higher d. However, we can still make some general observations.

First of all if it exists the horizon must have the topology of S^{d-2} since it is a surface of constant r. Further to avoid a naked singularity, we require the mass (*i.e.,* μ) to be positive. The latter can be deduced with two observations: first, the singularity appears at $r = 0$ and second, the function Π is everywhere positive (or zero) — recall the definition in eq. (1.13). Hence for eq. (1.21) to have a root at positive r, we must have $\mu > 0$. With a closer examination of the polynomial in eq. (1.21), we see that, in fact, it is large and positive for large $|r|$ and has a single minimum. Hence we conclude that there are only three possible scenarios: two, one or zero horizons. Hence in this regard, the higher dimensional metrics (1.11) are the same as the familiar Kerr metric in $d = 4$. However, an interesting difference arises if one (or more) of the spin parameters vanishes. Recall that Pi is monotonically increasing and grows as r^{2n} at large r. However, in this case, Π vanishes at $r = 0$ and grows as r^{2m} for small r, with m vanishing spin parameters. Hence the right-hand side of eq. (1.21) is negative for small r while it still becomes large and positive for large r. Hence there must always be one non-degenerate root at positive r, corresponding to a single horizon. This result holds irrespective of how large the remaining spin parameters are and hence the event horizon appears even when the angular momentum grows arbitrarily large, as long as there is no rotation in at least on of the orthogonal planes. These solutions with very large angular momenta have been dubbed 'ultra-spinning' black holes in [6]. As we will see in section 1.2.8, the latter have further interesting consequences.

For $d = 2n + 1$, the location of the horizon in eq. (1.14) is determined by

$$\Pi - \mu r^2 = 0\,. \tag{1.22}$$

It is more useful to present this expression using the new radial coordinate $\rho = r^2$ introduced in the previous discussion of singularities. In terms of ρ, eq. (1.22) becomes

$$\prod_{i=1}^{n}(\rho + {a_i}^2) - \mu\rho = 0\,. \tag{1.23}$$

Hence we are looking for the roots of a polynomial of order n and so analytic solutions only exist for $n = 2$, 3 and 4, *i.e.,* d=5, 7, 9 — these are given in Appendix B for $d = 5$. Of course, the horizon has the topology of S^{d-2} since it is a surface of constant ρ.[5] Finding a root with $\rho > 0$ again requires positive μ. In fact, a positive root requires

$$\mu > \sum_i \prod_{j\neq i} {a_j}^2\,, \tag{1.24}$$

which ensures that the coefficient of the linear term is negative in eq. (1.23). This constraint is necessary but not sufficient for the absence of a naked singularity. Provided that μ is sufficiently large, we will again only find one or two horizons with positive ρ, just as in the case of even d. Note that for odd d, a single vanishing spin parameter is insufficient to guarantee the existence of a horizon, since the constraint (1.24) remains nontrivial. However if two or more of the spin parameters vanish, eq. (1.23) has one positive root, as well as a root at $\rho = 0$. Further in this particular case, we can have regular ultra-spinning solutions where the event horizon appears even when the remaining spin parameters become arbitrarily large.

Recall that the singularity structure distinguished the case of odd d and all $a_i \neq 0$. In particular, in this case, the surface $\rho = 0$ is nonsingular and the geometry extends to negative values of ρ. To avoid naked singularities here, we only need that the outermost horizon, *i.e.,* the largest root of eq. (1.23), appears for $\rho > -a_s^2$ where the singularity appears.[6] Now with positive μ, the only possibility is that the horizon appears at positive ρ provided μ is sufficiently large, as described above. On the other hand, we have $\Pi(\rho = -a_s^2) = 0$ and hence for any negative μ, a root appears in eq. (1.23) in the range $-a_s^2 < \rho < 0$. Below, we will see that these negative mass solutions are even more pathological since they contain causality violating regions extending beyond the horizon. To close this discussion, we recall that when only one spin parameter has the minimal value, the geometry extends further to the range $-a_{s'}^2 < \rho < -a_s^2$. In this case, for small positive μ, one finds

[5] Implicitly we are assuming $\rho > 0$ here. See the additional discussion below of the case where all of the spin parameters are nonvanishing.

[6] As in the previous section, to discuss this case, we adopt the notation that a_s and $a_{s'}$ are the magnitudes of the smallest and second smallest spin parameters, respectively.

two roots or one degenerate root in this new range. However, these surfaces intersect the singular surface and so the latter is not entirely concealed by these horizons. Further if horizons occur in the range $-a_{s'}^2 < \rho < -a_s^2$, one may show no other horizons appear for positive ρ. Therefore these spacetimes contain naked singularities.

1.2.4 Ergosurfaces and Causality Violation

Turning now to ergosurfaces, we must determine the surfaces where g_{tt} vanishes. From the metrics in eqs. (1.11) and (1.14), the latter correspond to the roots of

$$\begin{aligned} F\Pi - \mu r &= 0\,, \qquad \text{even } d \\ F\Pi - \mu r^2 &= 0\,, \qquad \text{odd } d \end{aligned} \tag{1.25}$$

for $r > 0$. These surfaces still have the topology of S^{d-2} but, of course, the factor F introduces a more complicated directional dependence than appears for the horizons. As above, while there is no analytic solution for these equations, one is still able to deduce the general properties of the surfaces. In particular, one such surface always appears outside of the outer horizon and another may appear inside the inner horizon, if the latter exists. As can be seen from eq. (1.25), the ergosurface will touch the horizons where $F = 1$. If m spin parameters vanish when d is even, then the latter corresponds to the $(2m)$-dimensional sphere described by $1 = \alpha^2 + \sum_{k=1}^{m} \mu_k^2$, where the sum runs over the m indices for which $a_k = 0$. Hence if no spin parameters vanish, the two surfaces only touch at the two points on the horizon where $\alpha = \pm 1$, as found for the four-dimensional Kerr metric. Similarly if m spin parameters vanish when d is odd, the ergosurface and horizon will touch along the S^{2m-1} described by $1 = \sum_{k=1}^{m} \mu_k^2$. In particular, the two surfaces will not coincide anywhere if all of the spin parameters are nonvanishing in the case of odd d. Further in this case, one finds that with positive μ, there will be an ergosurface outside of the outer horizon but no such surface inside the inner horizon. On the other hand, if μ is negative, no ergosurfaces exist at all.

As described in Chapter 1, the outer ergosurface marks the boundary within which particles cannot remain at rest with respect to infinity. Further, the spinning black holes in higher dimensions can be mined with Penrose processes, just as in four dimensions. Another analogy with $d = 4$ arises in the scattering waves propagating in these geometries, which produces superradiance for the MP solutions as in the Kerr metric.

We close this section by turning to the question of causality violation. For

many of the black holes under consideration, we need only consider $r > 0$ and in this domain, the angular coordinates are perfectly well-behaved. The exceptional cases requiring additional consideration correspond to the black holes where all of the $a_i \neq 0$. First for even d, r can be extended to negative values in the second asymptotic region. In this region, the metric components $g_{\phi_i\phi_i}$ can become negative leading to closed time-like loops, as occurs in the Kerr metric. For odd d and all $a_i \neq 0$, the geometry extends beyond $r = 0$ to negative values of $\rho = r^2$. In this case for a each angle ϕ_i, eq. (1.14) gives

$$g_{\phi_i\phi_i} = (\rho + {a_i}^2)\left(1 + \frac{\mu {a_i}^2}{\Pi}\right) \tag{1.26}$$

in the plane $\mu_i = 1$. The above expression will become negative if the second factor has a zero, *i.e.,* for radii inside that where $\Pi + \mu {a_i}^2 = 0$. Now recall that with $\mu < 0$, the horizon arises at the root of eq. (1.23) which lies between $\rho = -a_s^2$ and 0. Hence the more important observation is that for any angle ϕ_i for which the corresponding spin parameter satisfies $a_i^2 > a_s^2$, the above metric component will be negative for some values of ρ outside of the horizon (since Π is a monotonically increasing function). That is, the negative mass solutions typically contain causality violating regions extending beyond the horizon — the only exception would be the case when all of the spin parameters are precisely equal. For completeness, we also note that in this case with $\mu > 0$ and a single a_i taking the value $\pm a_s$, there is the possibility that eq. (1.26) may vanish for $a_i = a_s$ in the range $-a_{s'}^2 < \rho < -a_s^2$.

1.2.5 Maximal Analytic Extension

In examining the maximal analytic extension of the solutions (1.11) and (1.14), one can use the usual techniques developed to study four-dimensional black holes and the results are essentially the same as for $d = 4$. In particular, one finds two separate extensions of the spacetime at each horizon, *i.e.,* an infalling coordinate patch which extends the geometry across the future horizon and an outgoing patch which smoothly traverses the past horizon. In the following, our discussion will focus on the case of even d and the extension of eq. (1.11). However, with the obvious changes, the same discussion is easily adapted to the case of odd d, as we briefly examine near the end of this section.

Towards the construction of the maximal analytic extension of these spacetime geometries, it is straightforward to construct Eddington-like coordi-

nates

$$dt = dt_\pm \mp \frac{\mu r}{\Pi - \mu r}\, dr\,, \qquad (1.27)$$
$$d\phi_i = d\phi_{\pm,i} \pm \frac{\Pi}{\Pi - \mu r}\, \frac{a_i\, dr}{r^2 + {a_i}^2}\,.$$

With these new coordinates, the metric (1.11) becomes

$$ds^2 = -dt_\pm^2 + dr^2 + \sum_{i=1}^{n} (r^2 + {a_i}^2)\left(d\mu_i^2 + \mu_i^2\, d\phi_{\pm,i}^2\right) + r^2\, d\alpha^2$$
$$\pm 2 \sum_{i=1}^{n} a_i\, \mu_i^2\, d\phi_{\pm,i}\, dr + \frac{\mu r}{\Pi F}\left(dt_\pm \pm dr + \sum_{i=1}^{n} a_i\, \mu_i^2\, d\phi_{\pm,i}\right)^2 \qquad (1.28)$$

Hence the metric is well-behaved in either coordinate system at the horizons, *i.e.,* $\Pi - \mu r = 0$. Of course, various metric components are still singular at $\Pi F/r = 0$ since the latter corresponds to a true curvature singularity. As can be seen from eq. (1.28), each of these coordinate systems are adapted to a particular family of radial geodesics following the null vectors

$$k_\pm^\mu \frac{\partial}{\partial x^\mu} = \frac{\partial}{\partial t_\pm} \mp \frac{\partial}{\partial r}\,. \qquad (1.29)$$

That is, the '+' and '–' coordinates are well-behaved along infalling and outgoing geodesics, respectively, which cross the horizons. Hence t_+ remains finite on the future horizon, where $r \to r_{\rm H}$ and $t \to +\infty$, while t_- remains finite on the past horizon, where $r \to r_{\rm H}$ and $t \to -\infty$.

The above Eddington-like coordinates (1.27) indicate that the structure of the horizons is essentially the same as that found in four dimensions. In particular, let us consider the case where eq. (1.21) has two distinct roots at positive r — recall this requires that all of the spin parameters are nonvanishing. Hence we have an outer event horizon at $r = r_{\rm H}$ and an inner Cauchy horizon at $r = r_{\rm C}$ ($< r_{\rm H}$). The corresponding Penrose diagram is shown in figure 1.1. A typical Eddington coordinate patch covers three regions in this diagram: the asymptotically flat exterior region where $r > r_{\rm H}$; the central region between the inner and outer horizons where $r_{\rm C} < r < r_{\rm H}$; and the inner region where $r < r_{\rm C}$ which contains a time-like "ring" singularity and which can be extended to an asymptotically flat region (with $r < 0$). If we consider the regions covered by the infalling coordinates $\{t_+, \phi_{+,i}\}$, then each of these three regions can be separately extended by transforming to the outgoing coordinates, $\{t_-, \phi_{-,i}\}$. Hence the maximally extended spacetime becomes a tower in which the basic geometry illustrated in figure 1.1 is repeated an infinite number of times. We might note that, as illustrated in

the figure, the horizons at $r = r_{\rm H}$ and $r_{\rm C}$ have the characteristic 'X' structure of a bifurcate Killing horizon. Here the various branches of the horizon are connected at the bifurcation surface at the center of the X, which corresponds to a fixed point of the associated Killing vector. Strictly speaking to demonstrate that the regions of the various overlapping Eddington patches are in fact smoothly connected at the bifurcation surface, one should find Kruskal-like coordinates, which are simultaneously well-behaved across both the future and past horizons (as well as the bifurcation surface). While this is certainly possible, the construction of these coordinates is a more involved exercise and we refer the interested reader to [1] for a discussion of this point.

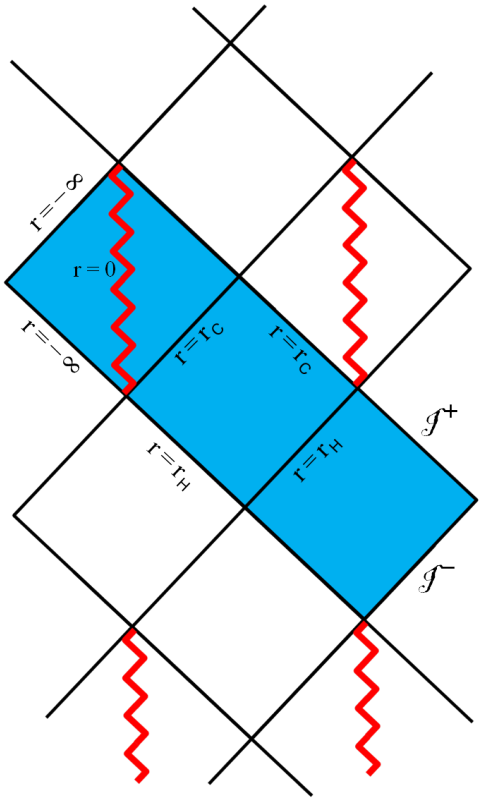

Figure 1.1 Penrose diagram for spinning black hole with two horizons for even d. The shaded regions indicate a single coordinate patch covered by infalling Eddington coordinates.

As noted above the inner horizon at $r = r_{\rm C}$ is a Cauchy horizon, representing the boundary for the unique evolution of initial data on some space-like

surface stretched across the Einstein-Rosen bridge joining two asymptotically flat regions. Now we expect that these Cauchy horizons should be unstable since the same simple arguments, which indicate such a surface is unstable in the four-dimensional Kerr metric, can be applied equally well here in higher dimensions. However, it must be said that this issue has not been studied in the same detail as in four dimensions and so an accurate description of the resulting singularity remains lacking for higher dimensions.

Above, we considered the spinning black holes (1.11) (with all of the $a_i \neq 0$) in the regime where there were two distinct horizons. Now if the mass of this solution is fixed and some of the spin parameters are increased, eventually the two horizons will coalesce producing an extremal black hole. In this case, the individual Eddington coordinate patches cover the exterior region and the inner region, and connecting these patches results in the maximal extension illustrated in figure 1.2(a). In this case, the near-horizon analysis of [7] can also be extended to higher dimensions to find that the throat region of the extremal black hole corresponds to an analog of the geometry $AdS_2 \times S^n$ [8]. If any of the spin parameters are further increased then the horizon disappears and one is left with a naked singularity, as shown in figure 1.2(b). Hence the extended black hole geometries described here and above provide a direct analogue in higher dimensions of the four-dimensional story for the Kerr solution, described in Chapter 1.

Another possibility, which we have not yet considered for even d, is when one or more of the spin parameters vanish. In this case, there is a single horizon but that it corresponds to a simple zero in eq. (1.21). There will be a second root but it occurs at the singularity at $r = 0$. One finds that this singular surface is space-like and so the Penrose diagram is similar to that of the Schwarzschild solution. In particular, there is no infinite tower of connected regions here but rather the singularities form space-like boundaries for the future and past interior regions. Here an analogy might be drawn with the $d = 4$ Kerr metric in the limit that $a \to 0$ where $r_{\rm C} \to 0$ and the geometry reduces to the Schwarzschild solution. However, in higher dimensions, there will in general still be other nonvanishing spin parameters but the structure of the spacetime remains unchanged irrespective of how large the remaining a_i become. Hence, as noted above, with one $a_i = 0$ (and d is even), we can construct ultra-spinning black holes carrying an arbitrary amount of angular momentum.

The above discussion was restricted to even d but there are no essential differences for the case of odd d. Of course as mentioned in section 1.2.2, with all of the spin parameters nonvanishing, the surface $r = 0$ is nonsingular and the geometry extends to negative values of $\rho = r^2$. Further one finds

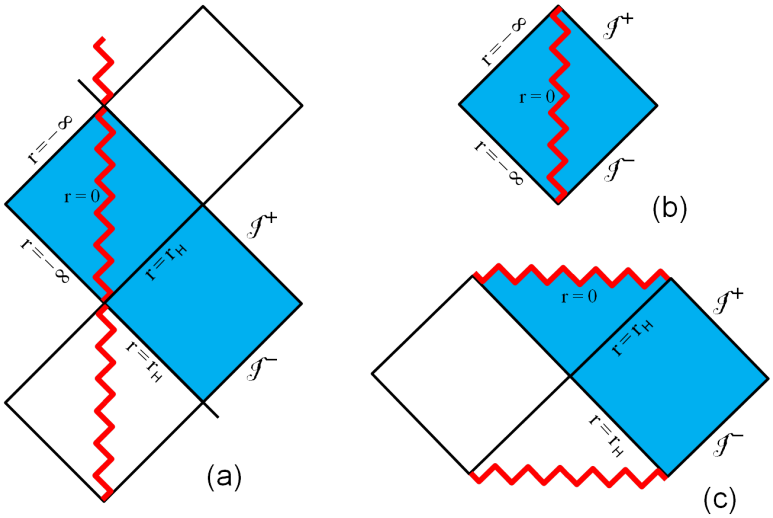

Figure 1.2 Further Penrose diagrams for even d: a) an extremal spinning black hole with single degenerate horizon, b) an over-rotating solution without horizon, and c) a spinning black hole with one or more $a_i = 0$. As before, the shaded regions indicate a single coordinate patch covered by infalling Eddington coordinates.

a time-like singularity in the latter domain but there is no connection to a second asymptotically flat region. Another difference is that the cases where the Penrose diagram takes a Schwarzschild form includes either two or more a_i=0 and $\mu > 0$ or one a_i=0 and $\mu > \sum_i \prod_{j\neq i} {a_j}^2$. The same structure also arises when all $a_i \neq 0$ and $\mu < 0$ but, as described above, these spacetimes are pathological since they contain causality violating regions outside of the horizon.

To close this section, let us make a few supplementary comments. First, we note that the metrics in eq. (1.28) actually have the so-called Kerr-Schild form

$$g_{\mu\nu} = \eta_{\mu\nu} \; + \; h\,(k_\pm)_\mu\,(k_\pm)_\nu \tag{1.30}$$

where $h = \mu r/\Pi F$. Of course, a further coordinate transformation would be required to introduce Cartesian coordinates so that the flat space line-element takes the conventional form. Here I might note that one of the remarkable features of the four-dimensional Kerr metric is that it can be written in this particular form [9]. Ultimately, it was the fact that the MP metrics can also be written in the Kerr-Schild form that allowed us to derive eqs. (1.11) and (1.14).

It is also interesting to examine the null vectors (1.29) in the original

coordinate system given in eq. (1.11):

$$k^\mu_\pm \frac{\partial}{\partial x^\mu} = \frac{\Pi}{\Pi - \mu r}\left(\frac{\partial}{\partial t} - \sum_{i=1}^{n} \omega_i \frac{\partial}{\partial \phi_i}\right) \mp \frac{\partial}{\partial r} \tag{1.31}$$

where $\omega_i = \frac{a_i}{r^2 + {a_i}^2}$. From these expressions, we see that upon approaching the horizon,

$$k^\mu_\pm \frac{\partial}{\partial x^\mu} \propto \frac{\partial}{\partial t} - \sum_{i=1}^{n} \Omega_i \frac{\partial}{\partial \phi_i}\,, \tag{1.32}$$

with $\Omega_i = \frac{a_i}{r_{\rm H}^2 + {a_i}^2}$. That is, k^μ_- becomes the generator of the future horizon at $r = r_{\rm H}$ in the infalling Eddington coordinate patch described by $\{t_+, \phi_{+,i}\}$. Similarly with infalling Eddington coordinates, k^μ_+ matches the generator of the past horizon at $r = r_{\rm H}$. A final comment is that these two vector fields given in eq. (1.29) or (1.31) correspond to the principal null vectors that appear in the algebraic classification, discussed in Chapter 9.

1.2.6 Hidden Symmetries and Geodesics

In the four-dimensional Kerr metric, particle motion is easily studied because the geodesics are completely soluble by quadratures. That is, there are four constants of motion, which allow us to write the complete solution for geodesic motion in terms of a set of indefinite integrals. At first sight, this is a rather remarkable property since the Killing symmetries and the fixed norm of the four-velocity only provide three such constants. The fourth constant is more subtle and relies on the existence of a Killing-Yano tensor in this particular background [10] – see below. The existence of this tensor is also responsible for the separability of the wave equation for spin-0, -1/2, -1 and -2 fields in this background. Recent work uncovered a rich structure of analogous relationships in higher dimensions, *e.g.,* [11, 12, 13, 14]. In particular, the required hidden symmetries were found for the Myers-Perry metrics [11], from which one can infer the integrability of geodesic motion in these backgrounds [12].

Central to this discussion is the existence of a rank-two closed conformal Killing-Yano tensor (CCKY) $h_{\mu\nu}$ which is a two-form satisfying

$$\nabla_{(\mu} h_{\nu)\rho} = \frac{1}{d-1}\left(g_{\mu\nu}\,\nabla_\sigma h^\sigma{}_\rho - \nabla_\sigma h^\sigma{}_{(\mu}\, g_{\nu)\rho}\right)\,. \tag{1.33}$$

As this two-form is closed, it also satisfies $dh = 0$ and so at least locally there exists a one-form potential b such that $h = db$. In the case of the MP

metrics, (1.11) and (1.14), the CCKY tensor can be explicitly written as

$$h = \sum_{i=1}^{n} a_i\, \mu_i\, d\mu_i \wedge \left(a_i\, dt + (r^2 + a_i^2)\, d\phi_i\right) + r\, dr \wedge \left(dt + \sum_{i=1}^{n} a_i\, \mu_i^2\, d\phi_i\right) . \tag{1.34}$$

Following the standard construction in four dimensions, one constructs a second-rank Killing tensor [10]

$$K_{(\mu\nu)} = -h_\mu{}^\sigma\, h_{\nu\sigma} + \frac{1}{2} g_{\mu\nu} h_{\rho\sigma} h^{\rho\sigma} \tag{1.35}$$

which then satisfies the identity

$$\nabla_{(\mu} K_{\nu\rho)} = 0\,. \tag{1.36}$$

It follows then that along a geodesic described by the d-velocity u^μ, the following is a constant of the motion: $K_{\mu\nu}\, u^\mu\, u^\nu$. In higher dimensions, the latter is only the first in a series of new conserved quantities. We will not describe the construction here but one finds the following tower of second-rank Killing tensors [11, 12]

$$K^{(\ell)\,\mu}{}_\nu = \frac{(2\ell)!}{(2^\ell\, \ell!)^2} \Big(\delta^\mu{}_\nu\, h^{[\mu_1\nu_1} \cdots h^{\mu_\ell\nu_\ell]} h_{[\mu_1\nu_1} \cdots h_{\mu_\ell\nu_\ell]} - 2\ell\, h^{\mu[\nu_1} \cdots h^{\mu_\ell\nu_\ell]} h_{\nu[\nu_1} \cdots h_{\mu_\ell\nu_\ell]}\Big) . \tag{1.37}$$

Note that comparing this expression to eq. (1.35), we see $K^{(1)}_{\mu\nu} = K_{\mu\nu}$. Now using eq. (1.33) for the CCKY tensor, it follows that all of these tensors satisfy the identity (1.36) and hence each provides a constant of the motion along a geodesic: $c_\ell = K^{(\ell)}_{\mu\nu}\, u^\mu\, u^\nu$.

From the above expression (1.37), it appears that this construction extends to $\ell = 1, \cdots, n+1$ for $d = 2n+2$. However, one finds that for $\ell = n+1$ that the right-hand side vanishes as an identity. On the other hand, one naturally extends this series to $\ell = 0$ with $K^{(0)\,\mu}{}_\nu = \delta^\mu{}_\nu$, in which case $c_0 = K^{(0)}_{\mu\nu}\, u^\mu\, u^\nu = g_{\mu\nu}\, u^\mu\, u^\nu$ is simply the norm of the d-velocity. Hence the Killing tensors then provide $n+1$ constants of motion. An essential feature of this construction is that these constants are in fact all independent. The latter statement is related to the fact that the CCKY tensor contains $n+1$ independent 'eigenvalues' for even d, when it is put in the standard form analogous to eq. (1.10). Of course, the Killing symmetries (time translations and the n rotations in each ϕ_i) provide a further $n+1$ constants of

the motion. Hence in total, there are $d = 2n + 2$ constants which allow us to solve for the geodesics in quadratures.

For $d = 2n + 1$, there is a similar counting of the constants of motion. In this case, the Killing tensors provide $n + 1$ independent constants c_ℓ with $\ell = 0, 1, \cdots, n$. Further the Killing symmetries provide $n + 1$ independent constants. At this point, it may seem that we have too many integration constants but, in the case of odd d, it turns out that c_n is reducible. That is, $c_{(n)} = (\xi^\nu \, g_{\mu\nu} \, u^\mu)^2$ where ξ^ν is a Killing vector [12]. This result is related to describing eq. (1.37) as the contraction of a CCKY tensor of rank $d-2\ell$ (dual to the wedge product of ℓ h's). Hence for $\ell = n$, the latter is a one-form for which the analog of eq. (1.33) reduces to Killing's equation. Hence this tensor is in fact simply a linear combination of the Killing vectors. Consequently, the total number of independent constants is precisely $d = 2n + 1$ and the geodesic motion is again completely integrable [12].

We comment that it has also been shown that the Killing(-Yano) tensors also lead to the separability of the Klein-Gordon and Dirac equations, as well as the Hamilton-Jacobi equations in these backgrounds, *e.g.,* [14]. While we do not have room to describe these results in detail here, a key element in this analysis is to construct 'symmetry operators' which commute with the appropriate wave operator. For example, in the case of the Klein-Gordon equation [13], we can start with simple operators constructed for each of the Killing coordinates, *i.e.,* $i\,\partial_t$ and $i\,\partial_{\phi_i}$, each of which commute with $\nabla^2 - m^2$. Various components of the separated solution of $(\nabla^2 - m^2)\psi = 0$ can then be identified as eigenfunctions of these operators, *e.g.,* $e^{i\omega t}$ and $e^{im\phi_i}$. Now the Killing tensors provide an additional set of symmetry operators: $\hat{K}^{(\ell)} = \nabla_\mu(K^{(\ell)\,\mu\nu}\nabla_\nu)$, which also satisfy $[\nabla^2 - m^2, \hat{K}^{(\ell)}]$. Again, various separated components of the desired solutions can then be written as eigenfunctions of these new operators. It remains an open question as to whether a similar set of symmetry operators can be constructed for the field equations of a Maxwell field or linearized gravitons and whether separability extends to these equations. We might note that some progress in analyzing linearized metric perturbations has been made for the particular case of odd d and all a_i equal [15].

1.2.7 Black Hole Thermodynamics

As already commented in chapter 1, the basic framework of black hole thermodynamics extends from four to higher dimensions in a straightforward way. We might add that implicitly this relies on the fact that our discussion of higher dimensional black holes is restricted to solutions of Einstein's

equations. There have also been interesting extensions of black hole thermodynamics to include both higher curvature actions and higher dimensions [16]. In any event, we will keep our comments here brief — see also comments in the following section.

The zeroth law, namely, that the surface gravity or temperature (*i.e.,* $T = \kappa/2\pi$) is constant across any stationary event horizon, is essential if the corresponding black holes are to behave like a thermal bath. This result is easily established if the horizon is a bifurcate Killing horizon, which is certainly the case here, following the discussion of section 1.2.5. As noted there, the horizon generator is given by

$$\chi^\mu \, \partial_\mu = \partial_t - \sum_{i=1}^{n} \Omega_i \, \partial_{\phi_i} \, . \tag{1.38}$$

Recall that $\Omega_i = \frac{a_i}{r_{\rm H}^2 + {a_i}^2}$. Hence using $\chi^\sigma \nabla_\sigma \chi^\mu = \kappa \chi^\mu$ to evaluate the surface gravity, one finds

$$\kappa = \begin{cases} \left. \frac{\partial_r \Pi - \mu}{2\mu r} \right|_{r=r_{\rm H}} & \text{for even } d \, , \\ \left. \frac{\partial_r \Pi - 2\mu r}{2\mu r^2} \right|_{r=r_{\rm H}} & \text{for odd } d \, . \end{cases} \tag{1.39}$$

While these are somewhat formal expressions, they clearly illustrate that κ is constant across the entire horizon.

Of course, the first law takes precisely the same form as in four dimensions:

$$\delta M = \frac{\kappa}{8\pi G} \, \delta \mathcal{A} + \sum_{i=1}^{n} \Omega_i \, \delta J_i \tag{1.40}$$

which leads to the interpretation of the area of (a cross-section of) the horizon $\mathcal{A}$ as the entropy of the black hole with the celebrated formula: $S = \mathcal{A}/4G$. (Of course, in an d-dimensional spacetime, this area $\mathcal{A}$ actually has the dimensions of length to the power $d-2$.) The Killing symmetries of the MP metrics also allow us to construct a useful related relation, known as the integrated Smarr formula [17],

$$\frac{d-3}{d-2} \, M = \sum_{i=1}^{n} \Omega_i \, J_i + \frac{\kappa}{8\pi G} \, \mathcal{A} \, . \tag{1.41}$$

Following [17], the irreducible mass of the black hole may be identified from the first law. This is the mass associated with the area of the horizon, *i.e.,* one integrates the area term in eq. (1.40),

$$M_{ir} = \frac{1}{8\pi G} \int_0^{\mathcal{A}} \kappa(\mathcal{A}', J_i = 0) \, d\mathcal{A}'$$

$$= \frac{d-2}{16\pi G}\,\Omega_{d-2}^{1/(d-2)}\,\mathcal{A}^{\frac{d-3}{d-2}}$$
$$= \frac{d-2}{d-3}\,\frac{\kappa\,\mathcal{A}}{8\pi G} \tag{1.42}$$

Hence $M - M_{ir}$ is the mass or energy connected to the rotation of the black hole and we expect that it may be removed through Penrose processes. In four dimensions, this can be explicitly verified because the geodesics in the Kerr metric are completely soluble by quadratures. Given the recent developments described in section (1.2.6), it would be interesting to extend this analysis to higher dimensions.

To close this section, we note that the second law (*i.e.,* $\delta\mathcal{A} \geq 0$) is also easily extended to higher dimensions, following the discussion in Chapter 1. One proof of the latter relies on the matter falling across the horizon satisfying the null energy condition and also on cosmic censorship [18]. While the former still seems a reasonable assumption in higher dimensions, the latter may appear more dubious given the recent results discussed in Chapter 3. However, the second law may also be proved by using the null energy condition and by demanding that the null generators of the horizon are complete [18]. In fact, the latter is consistent with our current understanding of the final state of the Gregory-Laflamme instability and hence it seems that the second law remains to have a firm foundation in higher dimensions.

1.2.8 Instabilities

While there is strong evidence for the stability of Kerr black holes in four dimensions, in fact, the opposite is true for spinning black holes in higher dimensions. That is, we believe that in higher dimensions, various instabilities arise for MP black holes when the angular momentum becomes large. In fact, it has been argued that these instabilities are related to the appearance of a rich fauna of new black holes in higher dimensions [19, 20].

A precise understanding of instabilities would require an analysis of the linearized perturbations of the MP metrics, (1.11) and (1.14). While this is possible in four dimensions, as noted in section 1.2.6, limited progress has been made in higher dimensions. However, insight into the situation in higher dimensions comes from making connections with the Gregory-Laflamme instability of black branes — see Chapter 2. As described below, this approach led to the conjecture that ultra-spinning black holes should be unstable for $d \geq 6$ [6] and numerical evidence of this conjecture was recently found [21, 22, 23]. An interesting consequence is that it seems that general

relativity in higher dimensions imposes a dynamical 'Kerr bound' on the spin of the form $J^{d-3} \lesssim GM^{d-2}$ in d dimensions.

To illustrate this point, let us consider the spinning black hole solutions with a single nonvanishing spin parameter. With this restriction, for either odd or even d, the metric reduces to

$$\begin{aligned} ds^2 = -dt^2 + \frac{\mu}{r^{d-5}\rho^2}\left(dt + a\sin^2\theta\, d\varphi\right)^2 + \frac{\Sigma}{\Delta}dr^2 \\ +\Sigma\, d\theta^2 + (r^2+a^2)\sin^2\theta\, d\varphi^2 + r^2\cos^2\theta\, d\Omega_{d-4}^2\,, \end{aligned} \tag{1.43}$$

where

$$\Sigma = r^2 + a^2\cos^2\theta \qquad \text{and} \qquad \Delta = r^2 + a^2 - \frac{\mu}{r^{d-5}}\,. \tag{1.44}$$

Here we have set $a_1 = a$ and $\mu_1 = \sin\theta$ (as well as $a_{i>1} = 0$). Now the event horizon is determined as the largest root r_{H} of $\Delta(r) = 0$. That is,

$$r_{\text{H}}^2 + a^2 - \frac{\mu}{r_{\text{H}}^{d-5}} = 0\,. \tag{1.45}$$

In examining this equation, it is not hard to see that for $d = 4$ or 5, there is an extremal limit (*i.e.,* an upper bound on a) beyond which no horizon exists. However, as our discussion in section 1.2.3 indicated, the more interesting case is $d \geq 6$. For the latter, we may note that the term r^2 makes the left-hand side of eq. (1.45) large and positive as $r \to \infty$. On the other hand, the term $-\mu/r^{d-5}$ makes $\Delta(r)$ negative for small r and hence there must be a (single) positive root independent of the value of a. That is, we have the possibility of ultra-spinning solutions, for which a regular event horizon remains even when the angular momentum (per unit mass) grows arbitrarily large.

Let us examine the geometry of the horizon of eq. (1.43) in this ultra-spinning regime. In the limit of very large a and fixed μ, the solution of eq. (1.45) is approximately given by

$$r_{\text{H}} \simeq \left(\frac{\mu}{a^2}\right)^{1/(d-5)} \ll a\,. \tag{1.46}$$

Hence we observe that r_{H} is shrinking as a grows (and μ is kept fixed). However, r_{H} is simply some coordinate expression and one must instead examine the horizon in a covariant way to uncover the true geometry. Various approaches may be taken here, all with the same simple result. If we characterize the size of the horizon along and orthogonal to the plane of rotation as $\ell_{\parallel}$ and $\ell_{\perp}$, respectively, then

$$\ell_{\parallel} \sim a \quad \text{and} \quad \ell_{\perp} \sim r_{\text{H}}\,. \tag{1.47}$$

That is, the horizon of these rapidly rotating black holes spreads out in the plane of rotation while contracting in the transverse directions, taking a 'pancake' shape in this plane. Considering the area of the horizon, we find

$$\mathcal{A} = \Omega_{d-2} r_{\rm H}^{d-4}(r_{\rm H}^2 + a^2) \simeq \Omega_{d-2} r_{\rm H}^{d-4} a^2 \simeq \Omega_{d-2} \left(\frac{\mu^{d-4}}{a^2}\right)^{1/(d-5)} . \qquad (1.48)$$

Note that the area decreases as a grows because the contraction in the transverse directions overcomes the spreading in the plane of rotation. We emphasize that this result (1.48) only applies for $d \geq 6$. The horizon area also decreases with increasing a in $d = 4$ or 5, but it is only for larger d that we can consider the ultra-spinning regime with $a \to \infty$, in which case the area shrinks to zero size.

Hence from the perspective of an observer near the axis of rotation and near the horizon (*i.e.,* near $\theta \sim 0$ and $r \sim r_{\rm H}$), the horizon geometry appears similar to that of a black membrane,[7] *i.e.,* it has roughly the geometry $R^2 \times S^{d-4}$. However, as we saw in Chapter 2, Gregory and Laflamme found that a black membrane would be classically unstable when the size in the brane directions is larger than that of the transverse sphere [24]. Hence it is natural to expect that the ultra-spinning MP solutions are unstable in the limit $a \to \infty$ but also that the instability actually sets in at some finite value of a [6].

The transition between the horizon behaving similar to the Kerr black hole and behaving like a black membrane is easily seen using black hole thermodynamics. One simple quantity to consider is the black hole temperature of the metric (1.43). Beginning from zero spin, T decreases as a grows, just like in the familiar case of the Kerr black hole. In $d = 4$ and $d = 5$ the temperature continues to decrease reaching zero at extremality, however, in $d \geq 6$ there is no extremal limit. So instead, T reaches a minimum and then starts growing again, as expected for a black membrane. The minimum, where this behavior changes, can be determined exactly [6]

$$\left.\frac{a^2}{r_{\rm H}^2}\right|_{crit} = \frac{d-3}{d-5} \qquad \text{or} \qquad \left.\frac{a^{d-3}}{\mu}\right|_{crit} = \frac{d-3}{2(d-4)} \left(\frac{d-3}{d-5}\right)^{\frac{d-5}{2}} . \qquad (1.49)$$

Following [21], we can use this critical ratio (1.49) to define the boundary of the ultra-spinning regime. That is, ultra-spinning solutions are defined to be those for which the ratio a^{d-3}/μ exceeds the critical value given in eq. (1.49). Explicitly evaluating eq. (1.49) for the latter ratio, we finds some

[7] This statement can be made mathematically precise in the limit $a \to \infty$ [6].

of these critical values to be

$$\left.\frac{a^{d-3}}{\mu}\right|_{crit} = 1.30,\ 1.33,\ 1.34,\ 1.35 \quad \text{for } d = 6,\ 7,\ 8,\ 9, \text{ respectively}\,. \quad (1.50)$$

We note that these critical values seem to be only weakly dependent on d. Further, these results would seem to indicate that the membrane-like behaviour, and hence the instability, arises for relatively small values of the spin parameter a.

A further connection to black hole thermodynamics appears because it is expected that the classical Gregory-Laflamme instabilities should be connected to thermodynamic instabilities of the corresponding black branes [25]. More precisely, it was conjectured that the appearance of a negative 'specific heat' for the black brane is connected to the appearance of this classical instability. Applying this reasoning in the present context would suggest that the rotating black hole should become unstable at some point after $\partial^2 S/\partial J^2 > 0$ [19], *i.e.,* after the point of inflection marked 'x' in figure 1.3. Given the expression for the area (1.48), one finds that this point corresponds precisely to that identified above from the behaviour of the temperature. That is, the critical point 'x' where $\partial^2 S/\partial J^2 = 0$ is given precisely by eq. (1.49).

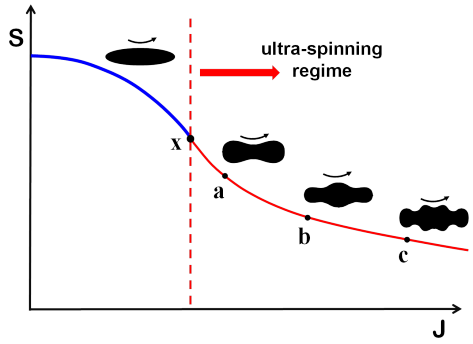

Figure 1.3 Phase diagram of entropy vs. angular momentum, at fixed mass, for MP black holes spinning in a single plane for $d \geq 6$. The point 'x' indicates where $\partial^2 S/\partial J^2 = 0$. The subsequent points (a,b,c, ...) correspond to the threshold of axisymmetric instabilities which introduce increasing numbers of ripples in the horizon. It is further conjectured that a new class of black holes with rippled horizons branches off from each of these points [19].

While resolving these issues analytically remains intractable at present, there has been remarkable progress coming from numerical investigations

in recent years [21]. If one considers the instability just at threshold, *i.e.,* precisely at the critical value of a, then the corresponding frequency is precisely zero and the unstable mode becomes a time-independent zero-mode. In [21], with a particular ansatz for such zero-modes, the authors were able to numerically locate the corresponding critical values of a for the singly spinning MP black holes (1.43) in $d = 6$ to 11. In fact, they found such a mode precisely where $\partial^2 S/\partial J^2 = 0$. However, the interpretation of this stationary mode is more subtle. Rather than corresponding to an instability, this perturbation simply corresponds to shifting the solution to a nearby MP black hole with a slightly larger spin. However, a small distance further into the ultra-spinning regime, they were also found a new zero-mode which 'pinches' the horizon at the axis of rotation, as illustrated for the point 'a' in figure 1.3. It is believed that this zero-mode does correspond to the onset of a true instability for higher values of the angular momentum J. Further, this was only the first of a hierarchy of zero-modes which introduced an increasing number of pinches or ripples in the event horizon along the θ direction. While these numerical searches only identified the stationary modes (by design), this provides strong evidence for a hierarchy of Gregory-Laflamme instabilities in the ultra-spinning regime.

These zero-modes also provide evidence for a new class of stationary rotating black holes with spherical horizons but with a rippled profile in the polar angle θ. The existence of these solutions was also conjectured in [6, 19]. According to the phase diagram suggested in [19], there would be a new branch of solutions beginning at the point 'a' and in moving along this branch, the pinch in the horizon at the axis of rotation would grow larger and larger. The conjecture is that this branch connects to yet another phase where the pinch produces a puncture in the horizon and the new phase would consist of spinning black rings, analogous to those discussed in Chapter 6 except the horizon topology would be $S^1 \times S^{d-3}$. Similarly, it is conjectured that the branch starting from the point 'b' would connect the spinning MP black holes to higher dimensional versions of the 'black saturn' found in [26] for five dimensions. Hence the new spinning black holes with rippled spherical horizons appear only to be a precursor to a rich fauna of new solutions with complex horizon topologies in higher dimensions

Implicitly, the latter analysis was only considering modes which respect all of the rotational symmetries present in the original metric (1.43), *i.e.,* $U(1) \times SO(d-3)$. However, this restriction was only imposed to simplify the analysis. A priori, there is no reason why all of the unstable modes should respect these symmetries. In fact, recent numerical studies suggest that non-symmetric modes play an important role in these instabilities. In

[23], full numerical simulations were carried out to describe evolution of rapidly spinning MP black holes in higher dimensions — again with a single nonvanishing spin parameter as in eq. (1.43). In all of the cases studied, it was found that the solutions were unstable against non-axisymmetric perturbations, with an initial profile proportional to $\sin(2\phi)$. The critical value where this 'bar-mode' instability set in was found to be:

$$\left.\frac{a^{d-3}}{\mu}\right|_{bar} = 0.76,\ 0.41,\ 0.28,\ 0.27 \quad \text{for } d = 5,\ 6,\ 7,\ 8, \text{ respectively}\,. \tag{1.51}$$

We should note that these values are considerably smaller than those identified above, in eq. (1.50). Notably, these numerical simulations were able to find an instability of the $d = 5$ MP black hole, where the previous discussion was unable to identify any instabilities. Further, following the nonlinear evolution of the unstable perturbation, the simulations [23] found that the deformed black holes spontaneously emit gravitational waves causing them to spin down and settle again to a stable MP black hole with a spin parameter smaller than the critical value in eq. (1.51). An open question is to determine when such 'bar-mode' instabilities arise for MP black holes rotating in more than one plane. As an aside, let us note here that in $d = 5$ with both spin parameters equal, it was shown analytically that no instabilities appear whatsoever [27].

In the preceding discussion, we have only considered MP black holes rotating in a single plane. However, this was only done to simplify the presentation and because this case was the focus of the numerical studies in [21, 23]. As discussed in section 1.2.3, ultra-spinning black hole solutions can also arise with several of nonvanishing spin parameters growing large, as long as one (or two) of the spin parameters vanish in even (or odd) d. It is natural to expect that the ultra-spinning regime also extends to the regime where several a_i grow large while the remainder stay small. Guided by this intuition, it is straightforward to extend the original discussion of the Gregory-Laflamme-like instabilities to the case where several spin parameters, say m, grow without bound while the remainder stay finite (or vanish) [6]. The limiting metric describes a (rotating) black $2m$-brane, where the horizon topology is $R^{2m} \times S^{d-2-2m}$. However, a Gregory-Laflamme-like instability is again expected to appear for these branes when the characteristic size in the planes with large spins is somewhat larger than the characteristic size in the transverse directions. In general, with many independent spins, the thermodynamic analysis mentioned above extends studying of the Hessian $\partial^2 S/\partial J_i \partial J_j$ for negative eigenvalues [21]. This expression provides a more refined definition of ultra-spinning black holes. In particular, following

the discussion with a single nonvanishing J_i, we define the boundary of the ultra-spinning regime as the boundary where this Hessian first acquires a zero eigenvalue.

Further insights into ultra-spinning instabilities have been found for one other example [20, 27, 28], namely, odd $d = 2n + 1$ with all of the n spin parameters equal. As noted, in section 1.2.1, the rotational symmetry of these geometries is enhanced to $U(n)$ and it can be shown that the metric involves a fibration over the complex projective space CP^n [15]. Further the metric perturbations of these spacetimes can be decomposed as harmonics on this CP^n and their analysis reduces to the study of an ordinary differential equation for the radial profile. Of course, in these metrics with all $a_i \neq 0$, there is an extremal limit and so it is not immediately obvious that one can reach an ultra-spinning regime or that any instabilities should appear. In fact, analysis of the above Hessian reveals an ultra-spinning regime for any odd $d \geq 7$. Ref. [20] explicitly identified unstable modes for $d = 9$ and supplementary work [28] later found unstable modes appeared very close to the extremal limit for $d = 7$, 9, 11 and 13. Ref. [27] was able to show that no instabilities arise for $d = 5$. Hence these results suggest that instabilities will arise in these cohomogeneity-one black hole spacetimes for any odd $d \geq 7$. Recently these instabilities of the cohomogeneity-one black holes were connected to those of the singly spinning black holes with the numerical work of ref. [22]. They showed that the ultra-spinning instabilities in these two sectors are continuously connected by examining perturbations of MP black holes with all but one of the spin parameters being equal. While their explicit calculations were made for $d = 7$, similar results are expected for higher odd d as well.

To close, we observe that the construction of the threshold zero-modes in $d = 9$ suggest that there should be a new family of spinning black hole solutions characterized by 70 independent parameters [20]!! Generically, these solutions would have only two Killing symmetries, *i.e.,* time translations and one $U(1)$ rotation symmetry. Hence here again, the ultra-spinning instabilities open the window on a exciting panorama of new black hole solutions in higher dimensions.

Acknowledgements

Research at Perimeter Institute is supported by the Government of Canada through Industry Canada and by the Province of Ontario through the Ministry of Research & Innovation. The author also acknowledges support from an NSERC Discovery grant and funding from the Canadian Institute for

Advanced Research. I would also like to thank the Aspen Center for Physics for hospitality while preparing this paper. I would also like to thank Roberto Emparan, Gary Horowitz, David Kubiznak and Jorge Santos for their comments on this manuscript.

Appendix A: Mass and Angular Momentum

This appendix will consider the definition of the mass and angular momentum of an isolated gravitating system in d dimensions. Our approach is to simply generalize the standard asymptotic analysis of four-dimensional solutions of Einstein's equations [29] to higher dimensions. In particular, the mass and angular momentum of any isolated gravitating system (*e.g.,* a black hole) may be defined by comparison with a system which is both weakly gravitating and non-relativistic. The result then provides the d-dimensional generalization of the ADM mass and angular momentum [29].

So let us begin with the d-dimensional Einstein equations

$$R_{\mu\nu} - \frac{1}{2} g_{\mu\nu} R = 8\pi G\, T_{\mu\nu}\,, \tag{1.52}$$

where we have included the stress-energy tensor for some matter fields, as it will be useful in the following discussion.[8] Now we wish to consider solutions of these equations when the gravitating system is both weakly gravitating and non-relativistic. First, with a weakly gravitating system, the metric is everywhere only slightly perturbed from its flat space form:

$$g_{\mu\nu} = \eta_{\mu\nu} + h_{\mu\nu}\,, \tag{1.53}$$

with $|h_{\mu\nu}| \ll 1$. Next, if the the system is non-relativistic, any time derivatives of fields will be much smaller than their spatial derivatives. Of course, this also implies that components of the stress energy tensor may be ordered

$$|T_{00}| \gg |T_{0i}| \gg |T_{ij}|\,. \tag{1.54}$$

These inequalities indicate that the dominant source of the gravitational field is the energy density while the momentum density provides the next most important source.

The solutions are most conveniently examined in the harmonic gauge

$$\partial_\mu \left(h^{\mu\nu} - \frac{1}{2} \eta^{\mu\nu} h^{\alpha}{}_{\alpha} \right) = 0\,. \tag{1.55}$$

[8] In the following, Greek indices run over all values $\mu, \nu = 0, 1, \ldots d-1$, while Latin indices only run over spatial values $i, j = 1, 2, \ldots d-1$.

With this choice, to leading order, the Einstein equations (1.52) can be written as

$$\begin{aligned}\nabla^2 h_{\mu\nu} &= -16\pi G\left(T_{\mu\nu} - \frac{1}{d-2}\eta_{\mu\nu}T^{\alpha}{}_{\alpha}\right)\\ &= -16\pi G\,\widetilde{T}_{\mu\nu}\end{aligned} \tag{1.56}$$

where ∇^2 is the ordinary Laplacian in flat d-dimensional space, *i.e.,* we have dropped the time derivatives of the metric perturbation. Note that $T^{\alpha}{}_{\alpha} \approx -T_{00}$ for non-relativistic sources. Eq. (1.56) is now readily solved with

$$h_{\mu\nu}(x^i) = \frac{16\pi G}{(N-2)\Omega_{d-2}}\int \frac{\widetilde{T}_{\mu\nu}(y^i)}{|\vec{x}-\vec{y}|^{d-3}}\, d^{d-1}y \tag{1.57}$$

where the integral extends only over the $(d-1)$ spatial directions. Recall that Ω_{d-2} denotes the area of a unit $(d$–$2)$-sphere, as given in eq. (1.3). Now evaluating eq. (1.57) in the asymptotic region far from any sources, we have $r = |\vec{x}| \gg |\vec{y}|$ and so we may expand the result as

$$h_{\mu\nu}(x^i) = \frac{16\pi G}{(d-3)\Omega_{d-2}}\,\frac{1}{r^{d-3}}\int \widetilde{T}_{\mu\nu}\, d^{d-1}y + \frac{16\pi G}{\Omega_{d-2}}\,\frac{x^k}{r^{d-1}}\int y^k\,\widetilde{T}_{\mu\nu}\, d^{d-1}y + \cdots \tag{1.58}$$

To simplify our results, we consider the system in its rest frame, which implies

$$\int T_{0i}\, d^{d-1}x = 0\,, \tag{1.59}$$

and we choose the origin to sit at the center of mass, which fixes

$$\int x^k\, T_{00}\, d^{d-1}x = 0,. \tag{1.60}$$

Now the total mass and angular momentum are defined as

$$M = \int T_{00}\, d^{d-1}x\,, \tag{1.61}$$

$$J^{\mu\nu} = \int (x^\mu T^{\nu 0} - x^\nu T^{\mu 0})\, d^{d-1}x\,. \tag{1.62}$$

One further simplification comes from the conservation of stress-energy, which reduces to $\partial_k T^{k\mu} = 0$ in the present case of interest and from which we can infer

$$\int x^\ell\, T^{k\mu}\, d^{d-1}x = -\int x^k\, T^{\ell\,\mu}\, d^{d-1}x\,. \tag{1.63}$$

Now this result, along with eqs. (1.59) and (1.60), allows us to simplify the angular momentum to

$$\begin{aligned} J^{0k} &= 0 \\ J^{kl} &= 2\int x^k\, T^{\ell\,0}\, d^{d-1}x\,. \end{aligned} \tag{1.64}$$

Applying these results to the expansion in eq. (1.58), we find that to leading order far from the system

$$\begin{aligned} h_{00} &\approx \frac{16\pi G}{(d-2)\Omega_{d-2}}\,\frac{M}{r^{d-3}}\,, \\ h_{ij} &\approx \frac{16\pi G}{(d-2)(d-3)\Omega_{d-2}}\,\frac{M}{r^{d-3}}\,\delta_{ij}\,, \\ h_{0i} &\approx -\frac{8\pi G}{\Omega_{d-2}}\,\frac{x^k}{r^{d-1}}J^{ki}\,. \end{aligned} \tag{1.65}$$

While these results were derived for a system which is both weakly gravitating and non-relativistic, the asymptotic behaviour of the metric will be the same for any isolated gravitating system. In particular then, we use these expressions to identify the mass and angular momentum of the black hole solutions discussed in the main text.

Appendix B: A Case Study of d=5

For $d = 5$ dimensions, we can write the metric (1.11) as

$$\begin{aligned} ds^2 = -dt^2 + \frac{\mu}{\Sigma}\left(dt + a\,\sin^2\theta\,d\phi_1 + b\,\cos^2\theta\,d\phi_2\right)^2 + \frac{r^2\Sigma}{\Pi - \mu r^2}\,dr^2 \\ +\Sigma\,d\theta^2 + (r^2+a^2)\sin^2\theta\,d\phi_1^2 + (r^2+b^2)\cos^2\theta\,d\phi_2^2 \end{aligned} \tag{1.66}$$

where

$$\Sigma = r^2 + a^2\cos^2\theta + b^2\sin^2\theta\,, \tag{1.67}$$

$$\Pi = (r^2+a^2)\,(r^2+b^2)\,. \tag{1.68}$$

Comparing our notation here to that in the main text, we have set $a_1 = a$, $a_2 = b$, $\mu_1 = \sin\theta$ and $\mu_2 = \cos\theta$.

Singularities: Now with some computer assistance, one can easily calculate the Kretchman invariant

$$R_{\mu\nu\rho\sigma}R^{\mu\nu\rho\sigma} = \frac{24\mu^2}{\Sigma^6}(4r^2 - 3\Sigma)\,(4r^2 - \Sigma)\,. \tag{1.69}$$

At $r = 0$, this expression yields

$$R_{\mu\nu\rho\sigma}R^{\mu\nu\rho\sigma}|_{r=0} = \frac{72\mu^2}{(a^2\cos^2\theta + b^2\sin^2\theta)^4}\,. \tag{1.70}$$

Hence if $b = 0$ above, we see there is a divergence as $\theta \to \pi/2$, as described in case (b) in section 1.2.2. Further with $b = 0$, if we examine (r, ϕ_2) part of the metric near $r = 0$ but away from $\theta = \pi/2$, we find

$$ds^2 \simeq \frac{\cos^2\theta}{1 - \frac{\mu}{a^2}}\left(dr^2 + \left(1 - \frac{\mu}{a^2}\right) r^2\, d\phi_2^2\right) + \cdots\,. \tag{1.71}$$

Hence we see that there is an angular deficit of $\Delta\phi_2 = 2\pi\mu/a^2$ on this axis.

On the other hand with both a and b nonvanishing, curvature invariant in eq. (1.70) remains finite. In this case, we introduce the radial coordinate $\rho = r^2$ and assuming $0 < a^2 \le b^2$, we find

$$R_{\mu\nu\rho\sigma}R^{\mu\nu\rho\sigma}|_{\rho=-a^2} = \frac{24\mu^2(4a^2 + 3(b^2 - a^2)\sin^2\theta)(4a^2 + (b^2 - a^2)\sin^2\theta)}{(b^2 - a^2)^6\,\sin^{12}\theta}\,. \tag{1.72}$$

Hence in accord with the discussion of case (c) in section 1.2.2, the surface $\rho = -a^2$ is entirely singular if $b^2 = a^2$. However, if $b^2 \neq a^2$, the singularity in eq. (1.72) only appears at $\theta = 0$. Thus in this case, we can extend the geometry into the region $-b^2 \le \rho \le -a^2$. However, one finds that for any value of ρ in this domain, there are singularities at

$$\sin^2\theta = \frac{|\rho| - a^2}{b^2 - a^2} \tag{1.73}$$

where $\Sigma = 0$.

Horizons: With $d = 5$, eq. (1.22) for the horizon becomes a quadratic equation in r^2 and the roots are given by the relatively simple expressions

$$\begin{aligned} 2{r_{\scriptscriptstyle \rm H}}^2 &= \mu - a^2 - b^2 + \sqrt{(\mu - a^2 - b^2)^2 - 4a^2b^2}\,, \\ 2{r_{\scriptscriptstyle \rm C}}^2 &= \mu - a^2 - b^2 - \sqrt{(\mu - a^2 - b^2)^2 - 4a^2b^2}\,. \end{aligned} \tag{1.74}$$

Therefore the existence of a horizon requires

$$\begin{aligned} \mu &\ge a^2 + b^2 + 2\,|\,a\,b\,| \\ M^3 &\ge \frac{27\,\pi}{32\,G}({J_1}^2 + {J_2}^2 + 2|\,J_1J_2|)\,. \end{aligned} \tag{1.75}$$

The definitions of the mass and angular momentum given by eq. (1.15) have been inserted to yield the second equation and we have defined $J_1 \equiv J^{y_1x_1}$ and $J_2 \equiv J^{y_2x_2}$. Hence there are no ultra-spinning black holes in $d = 5$.

Rather, if the angular momentum exceeds the above condition (1.75), the solution contains a naked 'ring' singularity without any event horizon.

Ergosurfaces: The equation for the ergosurface reduces to $\Sigma - \mu = 0$ or

$$r_{\text{E}}^2(\theta) = \mu - a^2\,\cos^2\theta - b^2\,\sin\theta^2\,. \tag{1.76}$$

When both a and b are nonvanishing, it is not hard to show that $r_{\text{E}}^2 > r_{\text{H}}^2$, *i.e.,* the ergosurface nowhere touches the horizon.

Cohomogeneity-One: It is also interesting to observe the simplifications that arise when $b = a$. First note that in this case, we have

$$\Sigma = r^2 + a^2\,, \quad \text{and} \quad \Pi = (r^2 + a^2)^2. \tag{1.77}$$

Further then, we see that the angular components in the second line of eq. (1.66) now combine to give $(r^2 + a^2)\,d\Omega_3^2$, *i.e.,* the round metric on a three-sphere. Hence this portion of the metric is symmetric under $SO(4) \simeq SU(2) \times SU(2)$. However, this symmetry does not survive for the full metric because there are other angular contributions in the first line of eq. (1.66). However these terms can be written in terms of the potential

$$A = i(\bar{z}_1\,dz_1 + \bar{z}_2\,dz_2) = \sin^2\theta\,d\phi_1 + \cos^2\theta\,d\phi_2\,, \tag{1.78}$$

where $z_1 = \sin\theta\,e^{i\phi_1}$ and $z_2 = \cos\theta\,e^{i\phi_2}$. Writing A in terms of these complex coordinates makes clear that the surviving symmetry is $U(1) \times SU(2) = U(2)$, as discussed in section 1.2.1. The metric (1.66) with $b = a$ is called cohomogeneity-one because after imposing this $U(2)$ symmetry, the metric components are entirely functions of the single (radial) coordinate r.

This enhanced symmetry also leads to a simplicity in other aspects of the geometry. For example, the Kretchman invariant (1.69) is now only a function of r,

$$R_{\mu\nu\rho\sigma}R^{\mu\nu\rho\sigma} = \frac{24\mu^2}{(r^2+a^2)^6}(r^2-3a^2)\,(3r^2-a^2) \underset{r\to 0}{\simeq} \frac{72\mu^2}{a^8}\,. \tag{1.79}$$

Hence the singularity at $\rho = -a^2$ in eq. (1.72) simplifies to

$$R_{\mu\nu\rho\sigma}R^{\mu\nu\rho\sigma}|_{\rho=-a^2+\varepsilon^2} = \frac{384\mu^2\,a^2}{\varepsilon^{12}}\,, \tag{1.80}$$

where we are assuming that $\varepsilon \ll a$. We might also note that for these black holes, the location of ergosurface (1.76) reduces to $r_{\text{E}}^2 = \mu - a^2$ and so the latter is now also independent of θ. Given this simple result, it is also a straightforward exercise to write

$$r_{\text{E}}^2 - r_{\text{H}}^2 = \frac{\mu}{2}\left(1 - \sqrt{1 - 4a^2/\mu}\right) > 0\,, \tag{1.81}$$

confirming that the ergosurface does not touch the horizon at any point in these cohomogeneity-one black hole spacetimes.

References

[1] R. C. Myers and M. J. Perry, "Black Holes in Higher Dimensional Space-Times," Annals Phys. **172** (1986) 304.

[2] W. Chen, H. Lu and C. N. Pope, "General Kerr-NUT-AdS metrics in all dimensions," Class. Quant. Grav. **23** (2006) 5323 [arXiv:hep-th/0604125].

[3] F.R. Tangherlini, "Schwarzschild Field in n Dimensions and the Dimensionality of Space Problem," Nuovo Cim. **77** (1963) 636.

[4] S. Hwang, "A Rigidity Theorem for Ricci Flat Metrics," Geometriae Dedicata **71** (1998) 5;
G. W. Gibbons, D. Ida and T. Shiromizu, "Uniqueness and nonuniqueness of static vacuum black holes in higher dimensions," Prog. Theor. Phys. Suppl. **148** (2003) 284 [arXiv:gr-qc/0203004].

[5] R. C. Myers, "Higher Dimensional Black Holes in Compactified Space-times," Phys. Rev. D **35** (1987) 455.

[6] R. Emparan and R. C. Myers, "Instability of ultra-spinning black holes," JHEP **0309** (2003) 025 [arXiv:hep-th/0308056].

[7] J. M. Bardeen and G. T. Horowitz, "The Extreme Kerr throat geometry: A Vacuum analog of $AdS_2 \times S^2$," Phys. Rev. D **60** (1999) 104030 [arXiv:hep-th/9905099].

[8] H. K. Kunduri, J. Lucietti and H. S. Reall, "Near-horizon symmetries of extremal black holes," Class. Quant. Grav. **24** (2007) 4169 [arXiv:0705.4214 [hep-th]];
P. Figueras, H. K. Kunduri, J. Lucietti and M. Rangamani, "Extremal vacuum black holes in higher dimensions," Phys. Rev. D **78** (2008) 044042 [arXiv:0803.2998 [hep-th]].

[9] R. P. Kerr, "Gravitational Field of a Spinning Mass as an Example of Algebraically Special Metrics," Phys. Rev. Lett. **11** (1963) 237.

[10] M. Walker and R. Penrose, Comm. Math. Phys. **18** (1970) 265;
R. Penrose, Ann. N. Y. Acad. Sci. **224** (1973) 125;
R. Floyd, "The dynamics of Kerr fields," PhD Thesis, London (1973).

[11] V. P. Frolov and D. Kubiznak, "Hidden Symmetries of Higher Dimensional Rotating Black Holes," Phys. Rev. Lett. **98** (2007) 011101 [arXiv:gr-qc/0605058].

[12] D. N. Page, D. Kubiznak, M. Vasudevan and P. Krtous, "Complete integrability of geodesic motion in general Kerr-NUT-AdS spacetimes," Phys. Rev. Lett. **98** (2007) 061102 [arXiv:hep-th/0611083];

P. Krtous, D. Kubiznak, D. N. Page and V. P. Frolov, "Killing-Yano Tensors, Rank-2 Killing Tensors, and Conserved Quantities in Higher Dimensions," JHEP **0702** (2007) 004 [arXiv:hep-th/0612029].

[13] A. Sergyeyev and P. Krtous, "Complete Set of Commuting Symmetry Operators for Klein-Gordon Equation in Generalized Higher-Dimensional Kerr-NUT-(A)dS Spacetimes," Phys. Rev. D **77** (2008) 044033 [arXiv:0711.4623 [hep-th]].

[14] V. P. Frolov, P. Krtous and D. Kubiznak, "Separability of Hamilton-Jacobi and Klein-Gordon Equations in General Kerr-NUT-AdS Spacetimes," JHEP **0702** (2007) 005 [arXiv:hep-th/0611245];
T. Oota and Y. Yasui, "Separability of Dirac equation in higher dimensional Kerr-NUT-de Sitter spacetime," Phys. Lett. B **659** (2008) 688 [arXiv:0711.0078 [hep-th]];
M. Cariglia, P. Krtous and D. Kubiznak, "Dirac Equation in Kerr-NUT-(A)dS Spacetimes: Intrinsic Characterization of Separability in All Dimensions," arXiv:1104.4123 [hep-th].

[15] H. K. Kunduri, J. Lucietti and H. S. Reall, "Gravitational perturbations of higher dimensional rotating black holes: Tensor perturbations," Phys. Rev. D **74** (2006) 084021 [arXiv:hep-th/0606076].

[16] R. M. Wald, "Black hole entropy is the Noether charge," Phys. Rev. D **48** (1993) 3427 [arXiv:gr-qc/9307038];
V. Iyer and R. M. Wald, "Some properties of Noether charge and a proposal for dynamical black hole entropy," Phys. Rev. D **50** (1994) 846 [arXiv:gr-qc/9403028];
T. Jacobson, G. Kang and R. C. Myers, "On Black Hole Entropy," Phys. Rev. D **49** (1994) 6587 [arXiv:gr-qc/9312023].

[17] L. Smarr, Phys. Rev. Lett. **30** (1973) 71.

[18] S. W. Hawking and G. F. R. Ellis, *The Large Scale Structure of Space-Time* (Cambridge University Press, 1973).

[19] R. Emparan, T. Harmark, V. Niarchos, N. A. Obers and M. J. Rodriguez, "The Phase Structure of Higher-Dimensional Black Rings and Black Holes," JHEP **0710** (2007) 110 [arXiv:0708.2181 [hep-th]].

[20] O. J. C. Dias, P. Figueras, R. Monteiro, H. S. Reall and J. E. Santos, "An instability of higher-dimensional rotating black holes," JHEP **1005** (2010) 076 [arXiv:1001.4527 [hep-th]].

[21] O. J. C. Dias, P. Figueras, R. Monteiro, J. E. Santos and R. Emparan, "Instability and new phases of higher-dimensional rotating black holes," Phys. Rev. D **80** (2009) 111701 [arXiv:0907.2248 [hep-th]];
O. J. C. Dias, P. Figueras, R. Monteiro and J. E. Santos, "Ultraspinning instability of rotating black holes," Phys. Rev. D **82** (2010) 104025 [arXiv:1006.1904 [hep-th]].

[22] O. J. C. Dias, R. Monteiro and J. E. Santos, "Ultraspinning instability: the missing link," JHEP **1108** (2011) 139 [arXiv:1106.4554 [hep-th]].

[23] M. Shibata and H. Yoshino, "Bar-mode instability of rapidly spinning black hole in higher dimensions: Numerical simulation in general relativity," Phys. Rev. D **81** (2010) 104035 [arXiv:1004.4970 [gr-qc]];
M. Shibata and H. Yoshino, "Nonaxisymmetric instability of rapidly rotating black hole in five dimensions," Phys. Rev. D **81** (2010) 021501 [arXiv:0912.3606 [gr-qc]].

[24] R. Gregory and R. Laflamme, "Black Strings And P-Branes Are Unstable," Phys. Rev. Lett. **70** (1993) 2837 [arXiv:hep-th/9301052]; "The Instability of charged black strings and p-branes," Nucl. Phys. B **428** (1994) 399 [arXiv:hep-th/9404071].

[25] S. S. Gubser and I. Mitra, "Instability of charged black holes in Anti-de Sitter space," arXiv:hep-th/0009126;
H.S. Reall, "Classical and thermodynamic stability of black branes," Phys. Rev. D **64** (2001) 044005 [arXiv:hep-th/0104071].

[26] H. Elvang and P. Figueras, "Black Saturn," JHEP **0705** (2007) 050 [arXiv:hep-th/0701035].

[27] K. Murata and J. Soda, "Stability of Five-dimensional Myers-Perry Black Holes with Equal Angular Momenta," Prog. Theor. Phys. **120** (2008) 561 [arXiv:0803.1371 [hep-th]].

[28] J. E. Santos, unpublished;
M. Durkee and H. S. Reall, "Perturbations of near-horizon geometries and instabilities of Myers-Perry black holes," Phys. Rev. D **83** (2011) 104044 [arXiv:1012.4805 [hep-th]].

[29] R. Arnowitt, S. Deser and C. Misner, "Canonical Variables for General Relativity," Phys. Rev. **117** (1960) 1595;
R. Arnowitt, S. Deser and C. Misner, "Energy and the Criteria for Radiation in General Relativity," Phys. Rev. **118** (1960) 1100;
R. Arnowitt, S. Deser and C. Misner, "Coordinate Invariance and Energy Expressions in General Relativity," Phys. Rev. **122** (1961) 997.